H1prelim-09-011 Submitted to

XVII International Workshop on Deep Inelastic Scattering, DIS2009, April 26-30, 2009, Madrid
Parallel Session **Diffraction and Vector Mesons**

Electronic Access: www-h1.desy.de/publications/H1preliminary.short_list.html

First measurement of the longitudinal diffractive structure function F_L^D at HERA

H1 Collaboration

Abstract

A first measurement of the longitudinal diffractive structure function F_L^D using the H1 detector at HERA is presented. The structure function is extracted from first measurements of the diffractive cross section at centre of mass energies $\sqrt{s}$ of 225 and 252 GeV, together with a new measurement at $\sqrt{s}$ of 319 GeV, using data taken in 2007 at high values of inelasticity y. The measured F_L^D is compared to predictions from NLO QCD fits to previous measurements of the inclusive diffractive DIS cross section.

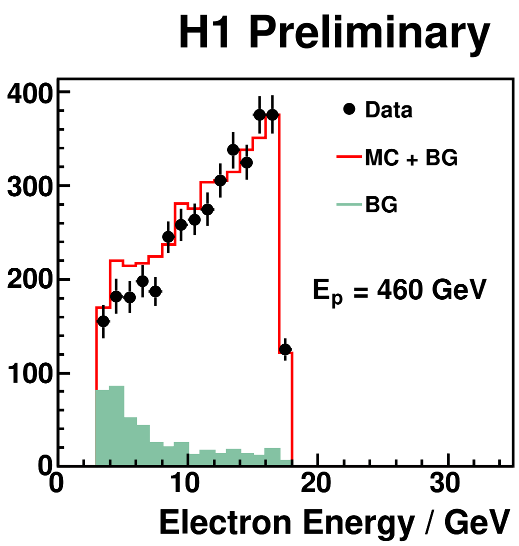

Figure 1: The electron energy distribution for $y_e > 0.38$ in the $E_p = 460$ GeV data. The positively-charged data events (points) are compared with the sum of negatively charged data events (green filled histogram) and diffractive DIS Monte Carlo which does not include F_L^D (red histogram).

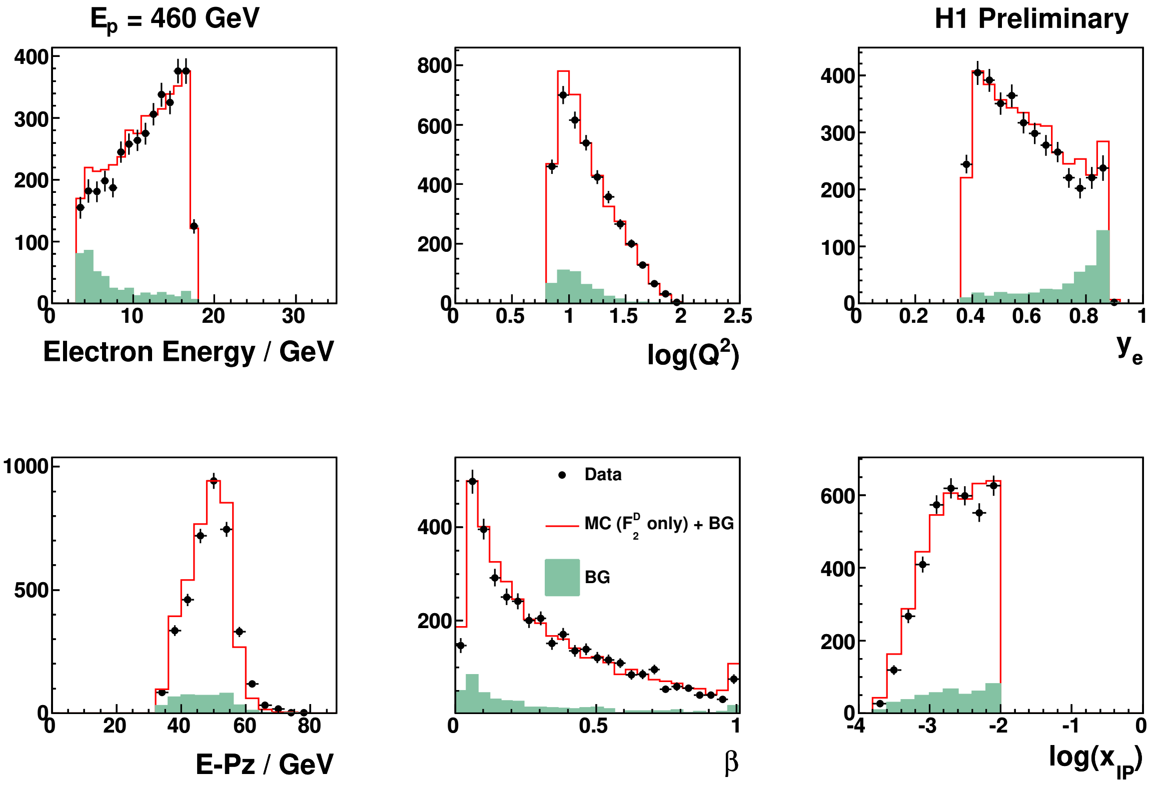

Figure 2: The electron energy, $log(Q^2)$, y_e, the summed $E - p_z$ of all final state particles, β and $x_{I\!P}$ distributions for the $E_p = 460$ GeV data, shown for $y > 0.38$. The positively-charged data events (points) are compared with the sum of negatively charged data events (green filled histogram) and diffractive DIS Monte Carlo which does not include F_L^D (red histogram).

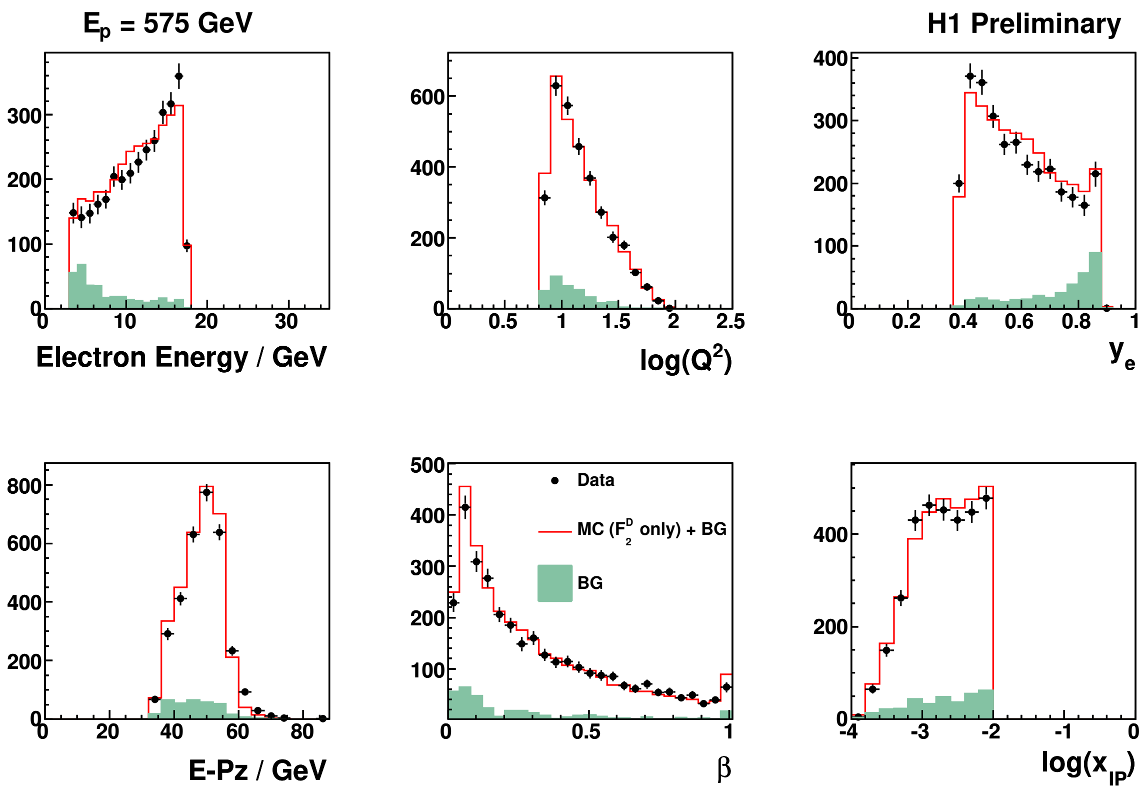

Figure 3: The electron energy, $log(Q^2)$, y_e, the summed $E - p_z$ of all final state particles, β and $x_{I\!P}$ distributions for the $E_p = 575$ GeV data, shown for $y > 0.38$. The positively-charged data events (points) are compared with the sum of negatively charged data events (green filled histogram) and diffractive DIS Monte Carlo which does not include F_L^D (red histogram).

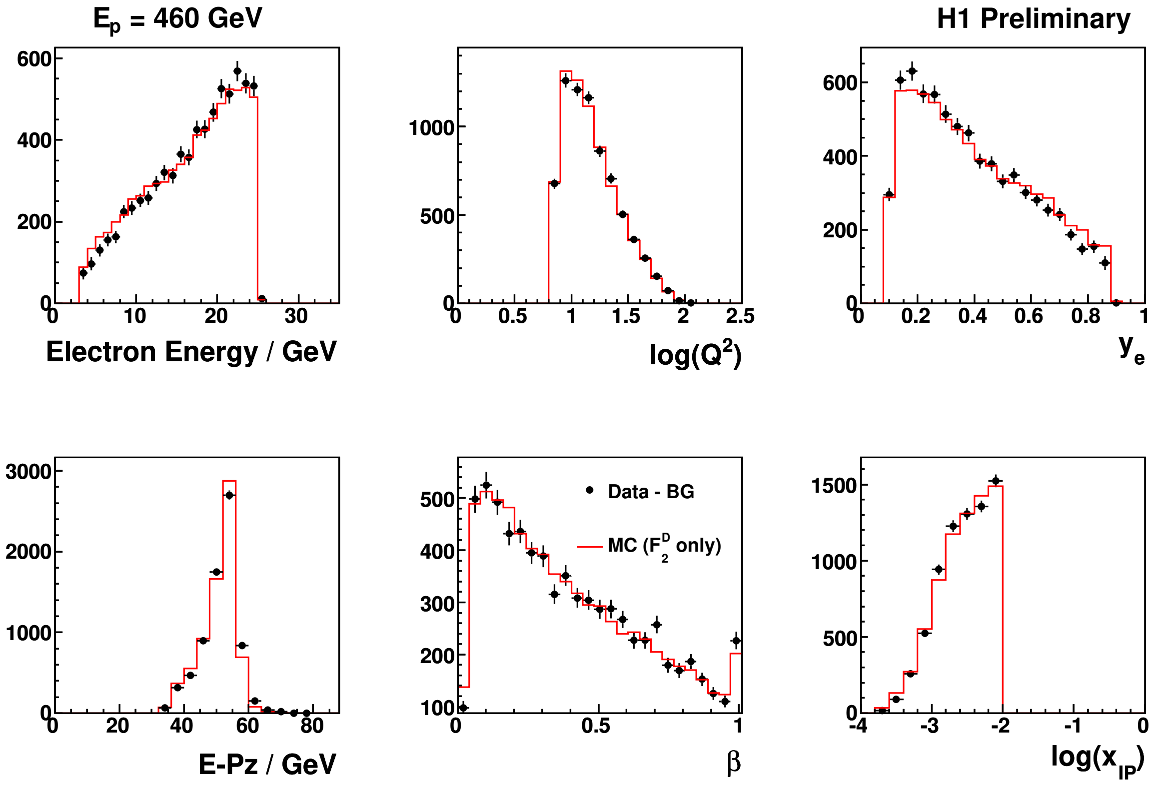

Figure 4: The electron energy, $log(Q^2)$, y_e, the summed $E - p_z$ of all final state particles, β and $x_{I\!P}$ distributions for the $E_p = 460$ GeV data, shown for all y. The positively-charged data events after subtraction of negatively charged events are shown as points, compared with diffractive DIS Monte Carlo which does not include F_L^D (red histogram).

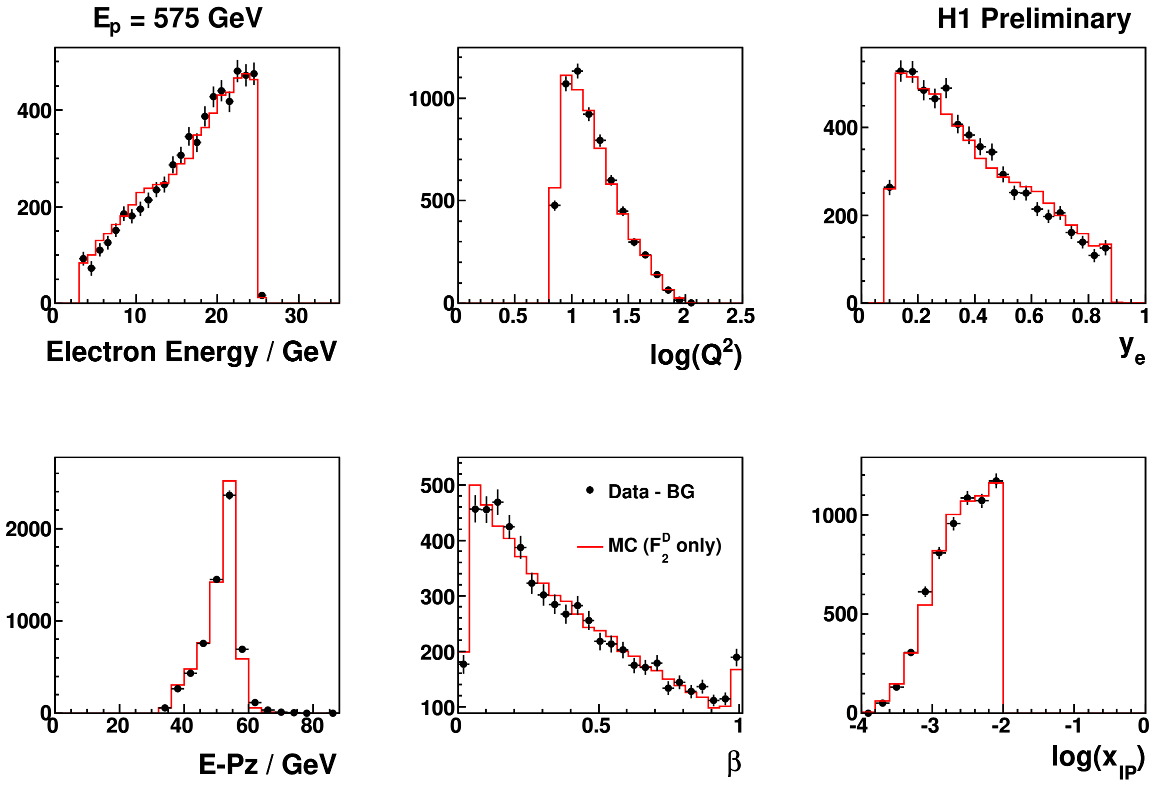

Figure 5: The electron energy, $log(Q^2)$, y_e, the summed $E - p_z$ of all final state particles, β and $x_{I\!P}$ distributions for the $E_p = 575$ GeV data, shown for all y. The positively-charged data events after subtraction of negatively charged events are shown as points, compared with diffractive DIS Monte Carlo which does not include F_L^D (red histogram).

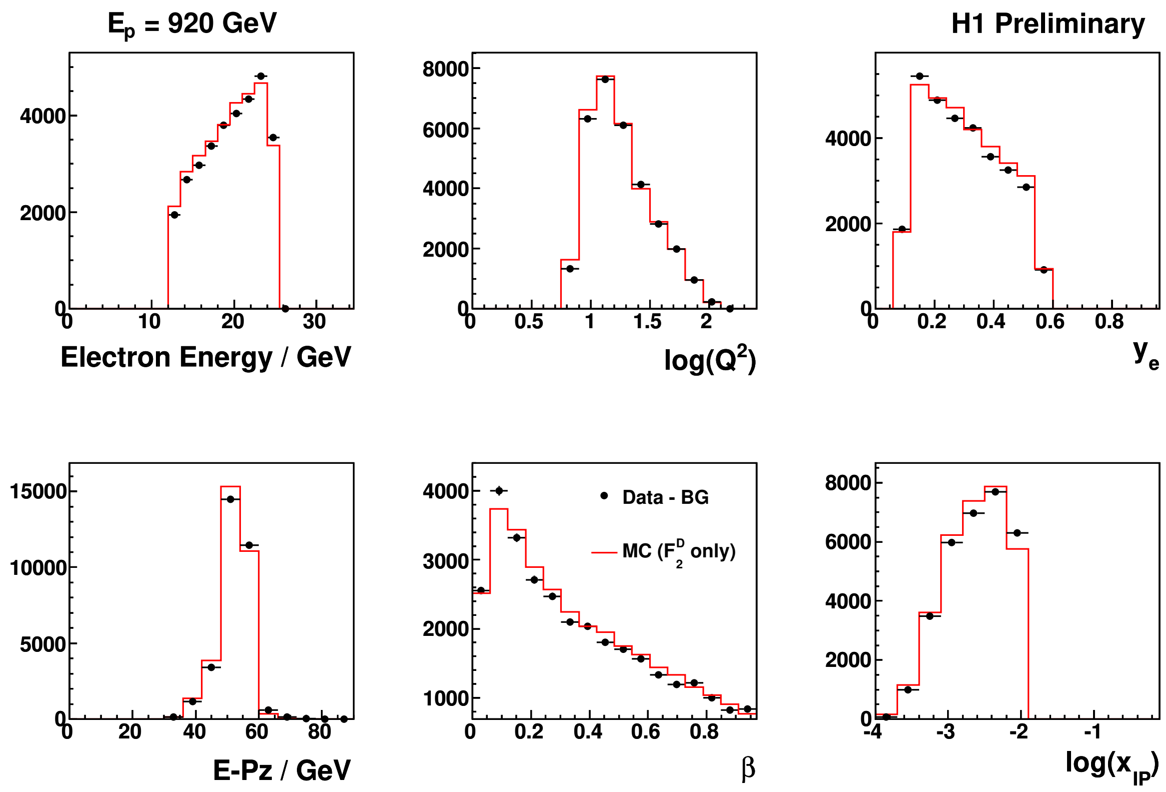

Figure 6: The electron energy, $log(Q^2)$, y_e, the summed $E - p_z$ of all final state particles, β and $x_{I\!P}$ distributions for the $E_p = 920$ GeV data, shown for all y. The positively-charged data events after subtraction of negatively charged events are shown as points, compared with diffractive DIS Monte Carlo which does not include F_L^D (red histogram).

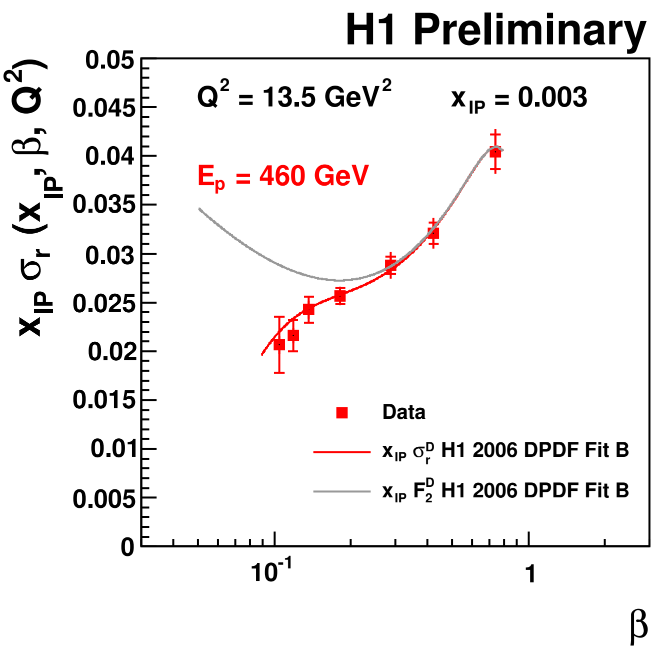

Figure 7: Measurement of the reduced cross section at $E_p = 460$ GeV. The data are compared to an NLO QCD fit to previous H1 data, H1 2006 DPDF Fit B. Also shown is the prediction for F_2^D from the same fit. The inner error bars are statistical, outer error bars show the statistical and systematic errors added in quadrature.

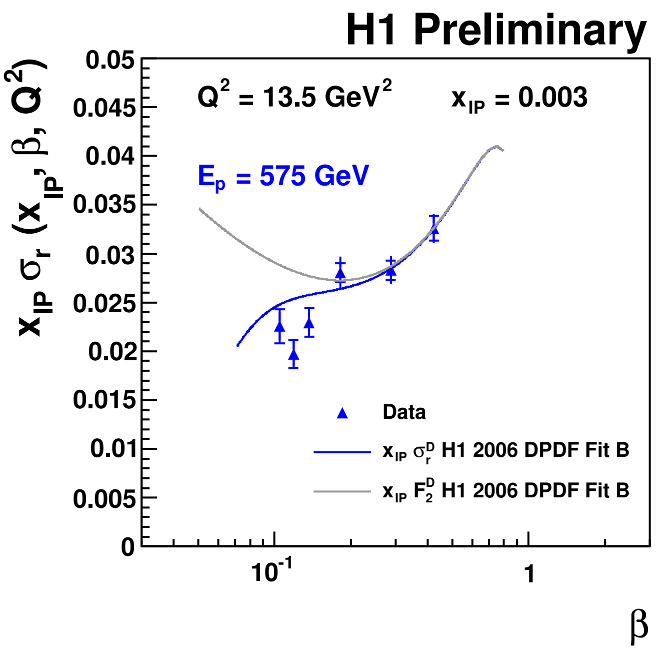

Figure 8: Measurement of the reduced cross section at $E_p = 575\ \mathrm{GeV}$. The data are compared to an NLO QCD fit to previous H1 data, H1 2006 DPDF Fit B. Also shown is the prediction for F_2^D from the same fit. The inner error bars are statistical, outer error bars show the statistical and systematic errors added in quadrature.

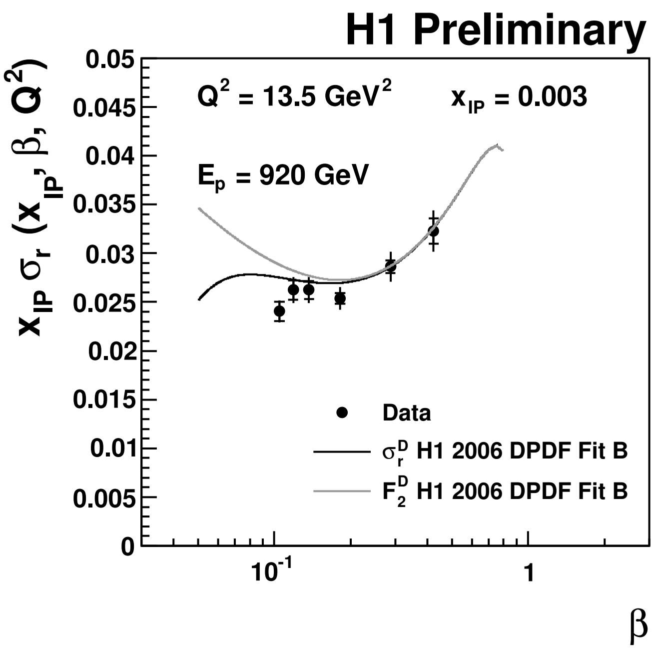

Figure 9: Measurement of the reduced cross section at $E_p = 920$ GeV. The data are compared to an NLO QCD fit to previous H1 data, H1 2006 DPDF Fit B. Also shown is the prediction for F_2^D from the same fit. The inner error bars are statistical, outer error bars show the statistical and systematic errors added in quadrature.

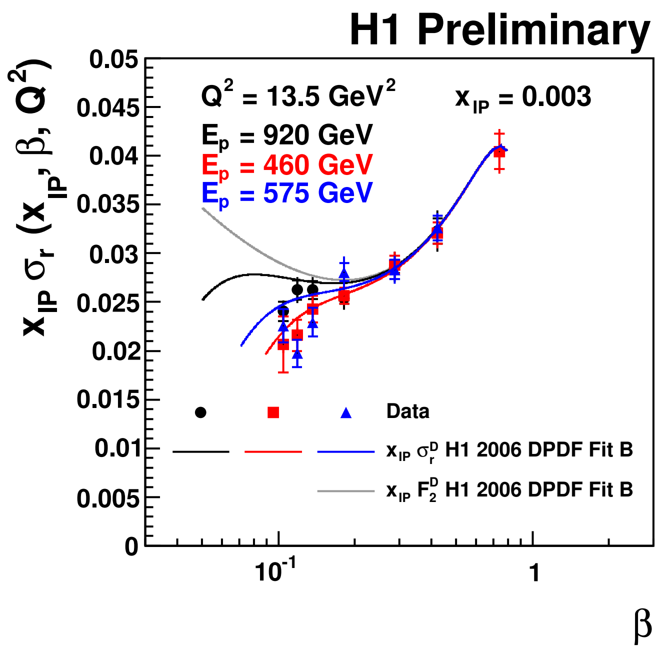

Figure 10: Measurement of the reduced cross section at $E_p = 460, 575$ and 920 GeV. The data are compared to an NLO QCD fit to previous H1 data, H1 2006 DPDF Fit B. Also shown is the prediction for F_2^D from the same fit. The inner error bars are statistical, outer error bars show the statistical and systematic errors added in quadrature.

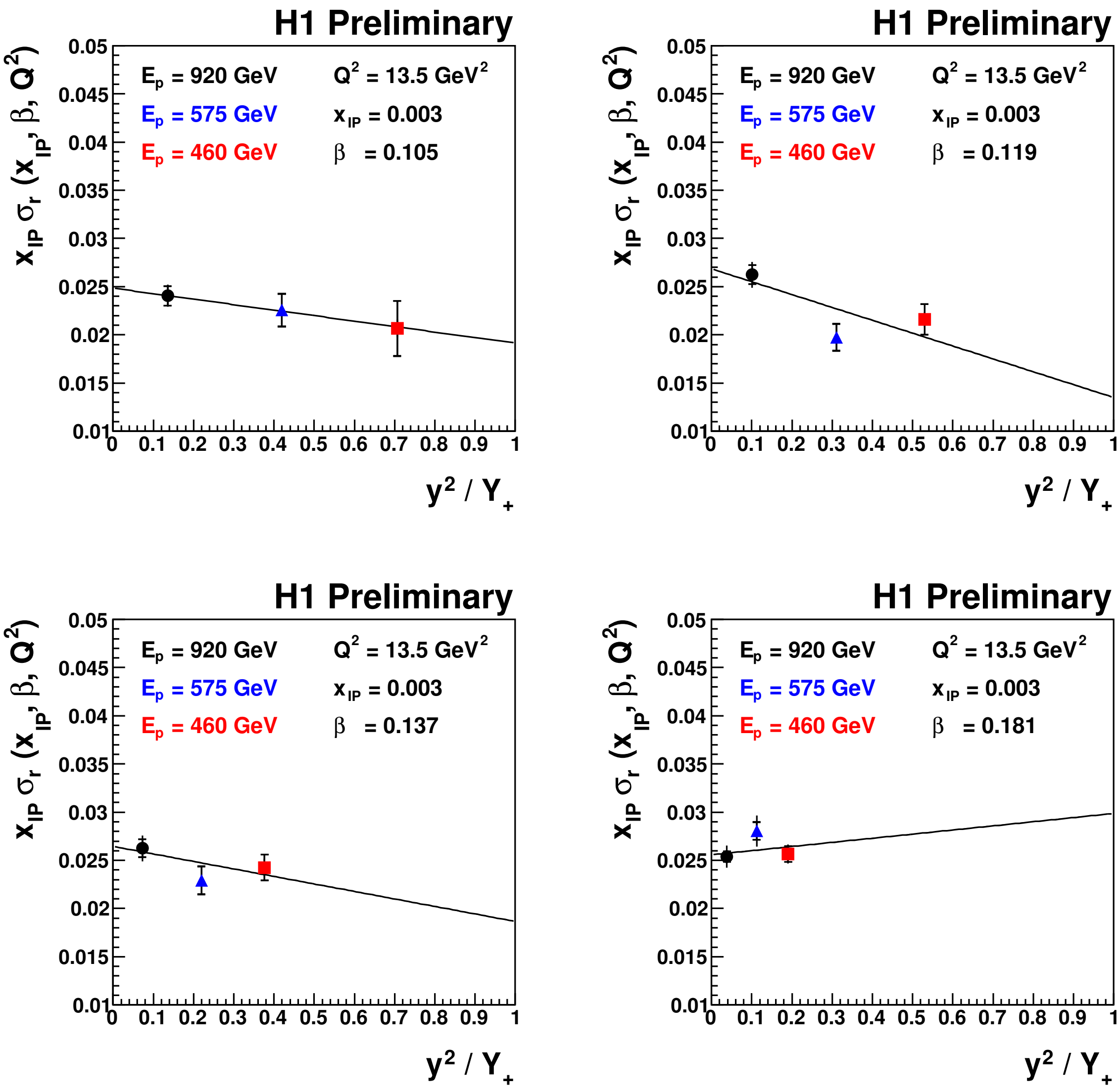

Figure 11: The reduced cross section measured at $Q^2 = 13.5\ GeV^2$ and different bins of β as a function of $y^2/[(1+(1-y)^2)]$ for $E_p = 460$ (red squares), $E_p = 575$ (blue triangles) and $E_p = 920$ (black circles) GeV. The inner error bars are statistical, outer error bars show the statistical and systematic errors added in quadrature. The straight lines show the linear fits used to determine F_L^D.

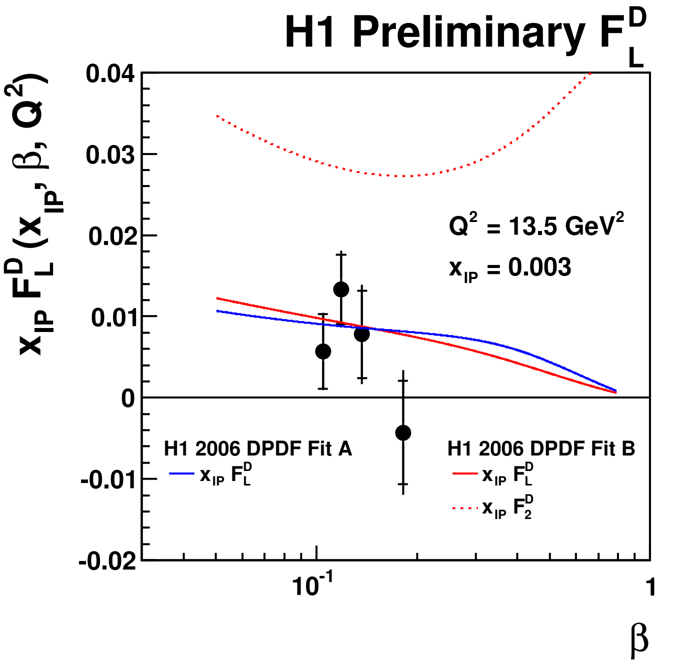

Figure 12: The diffractive longitudinal structure function F_L^D multiplied by $x_{I\!P}$. The data are compared to predictions from two NLO QCD fits to previous H1 data, H1 2006 DPDF Fit A (blue line) and Fit B (red line). The data are consistent with both predictions. Also shown is the value of F_2^D as a dashed red line.